Reaction Intermediates in the Solution Photochemistry of a Tetrarhodium Carbonyl Cluster: FTIR Structural Characterization and Transient Kinetics

D. V. Krupenya,[‡] E. O. Danilov,[†] M. A. J. Rodgers,*[,†] and S. P. Tunik*[,‡]

Center for Photochemical Sciences, Bowling Green State University, Bowling Green, Ohio 43403, and Department of Chemistry, St. Petersburg State University, Universitetskii pr., 26, St. Petersburg 198504, Russia

Received: April 18, 2003; In Final Form: July 21, 2003

The photochemistry of the tetranuclear rhodium carbonyl cluster, $Rh_4(CO)_{12}$, in heptane solution has been studied using pulsed laser photoexcitation coupled to time-resolved step-scan FTIR spectrometry. It was found that excitation of the cluster with 266 nm light results in CO dissociation to form a $Rh_4(CO)_{11}$(Solv) species, transformations of which were observed in the nanosecond time domain. Monitoring the reaction course revealed the presence of two successive transients, I and II, which eventually reform the parent cluster. The FTIR spectrometric study showed that these transients represent two isomeric forms of the $Rh_4(CO)_{11}$(Solv) species. The second transient exhibits the structure typical of ground-state substituted $Rh_4(CO)_{11}$(L) derivatives with the solvent molecule in an axial position of the basal plane of the metal tetrahedron. The first isomer is a "nonequilibrium" form of the same species where the solvent molecule occupies either a radial site at the basal rhodium triangle or a vacancy at the apical rhodium atom. The kinetics of the reaction sequence is consistent with a unimolecular isomerization of I into II and trapping of the latter by CO evolved at earlier stage of reaction. In the presence of excess CO in the reaction mixture the first transient is effectively scavenged to form $Rh_4(CO)_{12}$. The kinetic parameters of the isomerization process and the trapping of I by CO have been determined.

Introduction

Transition metal clusters remain somewhat unusual and intriguing chemical entities in organometallic chemistry. The presence of several metal atoms in the coordination core of the clusters provides structural complexity and extreme diversity in their chemical reactivity. Up to now advances in the synthesis and the structural characterization of metal clusters in solid state and in solution has prevailed over progress in investigations of their reactivity and reaction mechanisms. The most recent reviews in the field demonstrate this imbalance in knowledge of metal cluster chemistry.[1] This is particularly evident in their photochemical properties where most information has been obtained for simplest tri- and tetrametal clusters. The mechanistic features of photochemical transformations occurring in these polynuclear complexes have been studied either by the matrix isolation technique[2−5] or by a photokinetic approach based on the treatment of quantum yield dependence on the concentration of reaction components.[6−12] These days, direct information about the chemical behavior of transient species formed after photoexcitation can be obtained by flash photolysis experiments. However, quantitative data of this sort are rarely found in the transition metal cluster literature.[9,13,14] To some extent this lack of information about transient species formed after photoexcitation of the polynuclear complexes is due to the fact that the UV−vis probe techniques commonly used in flash photolysis experiments carry minimal structural information. On the other hand, time-resolved IR spectrometry is able to provide not only kinetic information but also much more detailed and valuable data concerning coordination sphere structure. This becomes particularly relevant to carbonyl complexes owing to the relatively high extinction coefficient of the carbonyl functionality and the sensitivity of the spectral bands to the symmetry of carbonyl environment. Transient IR spectrometry is capable of significantly impacting the amount and quality of structural and mechanistic information on the photochemical processes in mono-[15−17] and polynuclear carbonyl compounds.[2,3,5,14,18] The application of time-resolved step-scan FTIR spectroscopy in investigations of the photochemistry of organic compounds containing carbonyl groups such as the alkyl phenylglyoxylates[19] has clearly demonstrated the value of this approach and in this paper we present the results of structural characterization and nanosecond kinetic data for transients generated by photoexcitation of a tetranuclear rhodium carbonyl cluster, $Rh_4(CO)_{12}$, in a hydrocarbon solvent.

Experimental Section

Materials. Anhydrous heptane was purchased from Aldrich, and $Rh_4(CO)_{12}$ from Strem. Both were used without further purification.

Flash Photolysis Experiments. Details of the nanosecond TRFTIR spectrometer have been published.[19] All measurements were carried out at 20 °C. In a typical experiment, a saturated solution of $Rh_4(CO)_{12}$ in heptane (2.1 mM, 20 °C) was circulated by a peristaltic pump from a buffer vessel through a 0.2 mm path length flow cell with CaF_2 windows. The laser excitation beam (355 or 266 nm, ca. 10 mm in diameter) with energy up to 15 mJ per pulse was directed to the sample cell where it overlapped the infrared probe beam. This latter covered the 1350−2350 cm^{-1} interval (4 cm^{-1} resolution). The sample cell was positioned in the sample compartment of a Bruker "Equinox" step scan FTIR spectrometer, modified for nanosecond time resolution. Two regimes of the data acquisition were

[†] Bowling Green State University.
[‡] St. Petersburg State University.

10.1021/jp035050f CCC: $25.00
Published on Web 09/17/2003

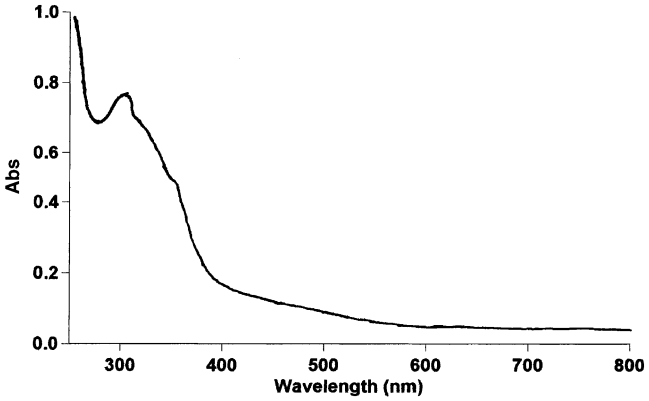

Figure 1. UV−vis spectrum of $Rh_4(CO)_{12}$ in heptane solution.

used. In the short time experiments (10 μs time window) 500 IR spectra were acquired every 20 ns after a laser pulse. In the slower time domain the time interval between acquisitions was 500 ns (250 μs time window). The stability of the $Rh_4(CO)_{12}$ solution under the exposure conditions was controlled by measuring the IR spectrum before and after completion of the experiment. No significant decomposition of the sample was detected.

In the experiments requiring variable CO concentrations, solutions were presaturated with standard CO/Ar gas mixtures for 15 min. The same gas mixture was bubbled through the buffer vessel to keep the CO concentration constant during the course of the experiment. The concentration of CO in solution was calculated using the literature data on CO solubility in heptane.[20]

Results

The UV−vis spectrum of $Rh_4(CO)_{12}$ in heptane, Figure 1, consists of an intense short wavelength ultraviolet absorption (λ_{max} < 200 nm) with two longer wavelength shoulders localized at 303 and 330 nm. In an earlier study[21] of the UV−vis spectra and electronic structure of $Rh_4(CO)_{12}$, the short wavelength absorption was assigned to an MLCT transition and the shoulders arose from $\sigma-\sigma^*$ transitions between metal−metal bonding and antibonding orbitals. It has been reported that in trinuclear carbonyl clusters of the iron subgroup, excitation in the MLCT band results in CO dissociation, whereas excitation in the $\sigma-\sigma^*$ band generated intermediates with a broken metal−metal bond.[2,3,8,11]

In our experiments, excitation of the $Rh_4(CO)_{12}$ solutions in heptane (see Experimental Section) with 266 nm or with 355 nm laser pulses showed no qualitative differences in the spectroscopic and kinetic characteristics of the transients observed except that signal amplitudes were higher using the former wavelength. Therefore, 266 nm excitation was used throughout to optimize the signal-to-noise ratio in the FTIR difference spectra. In a typical experiment, spectra in the 1800−2100 cm^{-1} range were acquired every 20 ns within a time window of 10 μs. A perspective view of a typical dynamic surface, $A(\bar{\nu},t)$, is shown in Figure S1 (Supporting Information). Immediately after the laser pulse the IR spectrum showed depletion of the $Rh_4(CO)_{12}$ cluster ground-state absorption (bleaching of the 2074, 2042, and 1886 cm^{-1} bands) accompanied by positive absorption bands at 2054, 2036, 2009, 1902, and 1866 cm^{-1}, corresponding to the first transient (I), see Figure 2. These bands reached their maximum amplitude within the time resolution of the instrument (ca 20 ns). Subsequent decay of the bands assigned to transient I was accompanied by growth of a spectral pattern characterized by absorptions at 2093, 2060, 2037, 2027, 2014, 1876, and 1858 cm^{-1}. These bands are attributed to transient II (Figure 3). The conversion of the spectral pattern of I in to that of II was not accompanied by any repopulation of the ground-state bleaching bands (Figures 3 and 4).

The kinetic properties of transients I and II were followed by extracting the time profiles at 2054 and 2061 cm^{-1}, respectively (Figure 4), from the data array. Averaging the data obtained in three experiments gave rate constants of $(4.8 \pm 0.1) \times 10^5$ and $(5.2 \pm 0.2) \times 10^5$ s^{-1} for the decay at 2054 cm^{-1} and the growth at 2061 cm^{-1}, respectively, when the time profile for the growth of II was corrected for its subsequent decay (see Figure 5). The close similarity of these decay and growth rate constants is indicative that transient II is a product of the decay of I and during this conversion there is no regeneration of the starting material.

With excess CO present in the sample, the time-resolved FTIR spectra showed a rapid conversion of I into $Rh_4(CO)_{12}$ without formation of appreciable amount of the transient II. This trapping of transient I by dissolved CO (even at somewhat low CO concentration) made it impossible to follow the reaction between

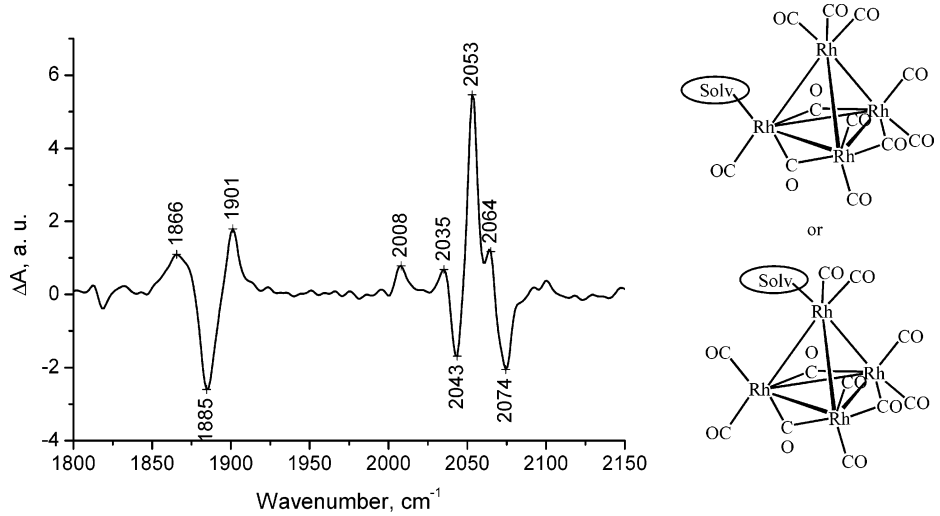

Figure 2. Infrared spectrum obtained by averaging the first 10 slices in a short time TR IR experiment (10 μs duration). Two structures shown in the figure schematically present possible locations of the solvent molecule in transient I (see text).

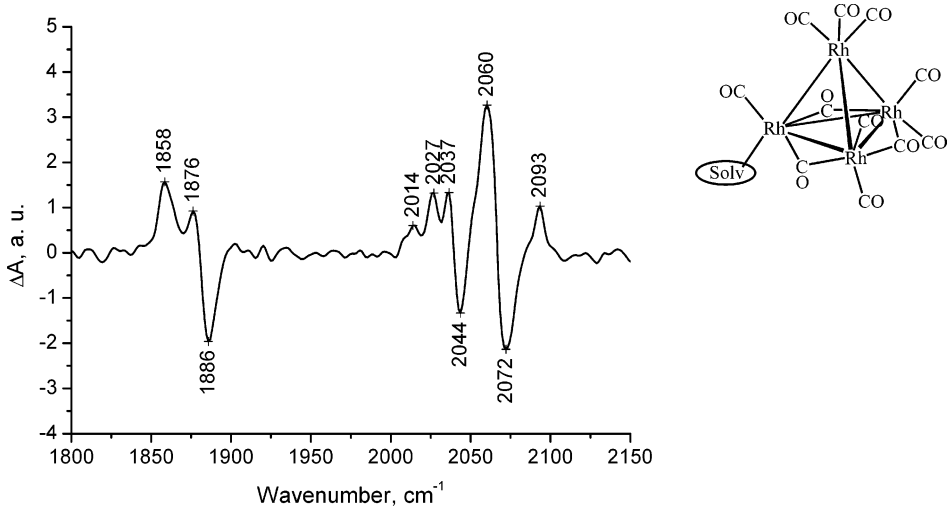

Figure 3. Infrared spectrum obtained by averaging the last 10 slices in a short time TR IR experiment (10 μs duration). The structure shown in this figure schematically presents locations of the solvent molecule in transient II (see text).

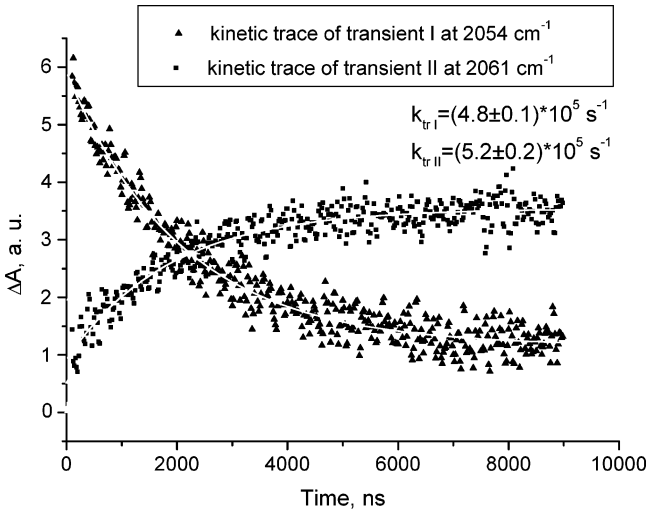

Figure 4. Time profiles of transient I (2054 cm^{-1}) and transient II (2061 cm^{-1}).

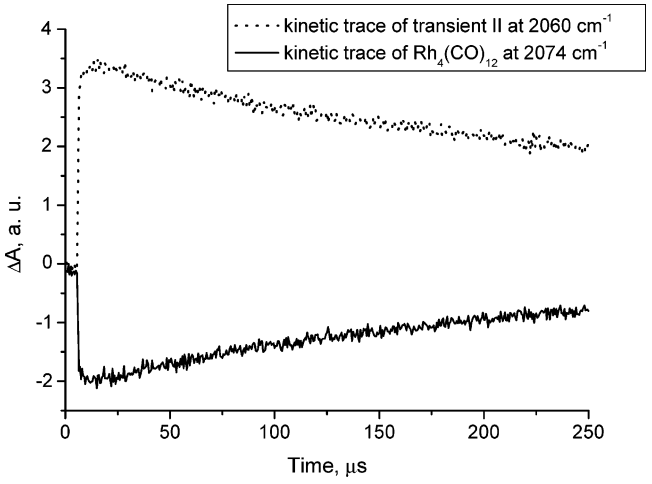

Figure 5. Time profiles of transient II (2060 cm^{-1}) and $Rh_4(CO)_{12}$ (2074 cm^{-1}).

CO and transient II. Nevertheless the bimolecular reaction of I with CO under first-order conditions was followed by measuring the rate constant (k_{obs}) for the decay of I at 2054 cm^{-1} as a function of [CO]. A plot of k_{obs} vs [CO] is shown in Figure 6

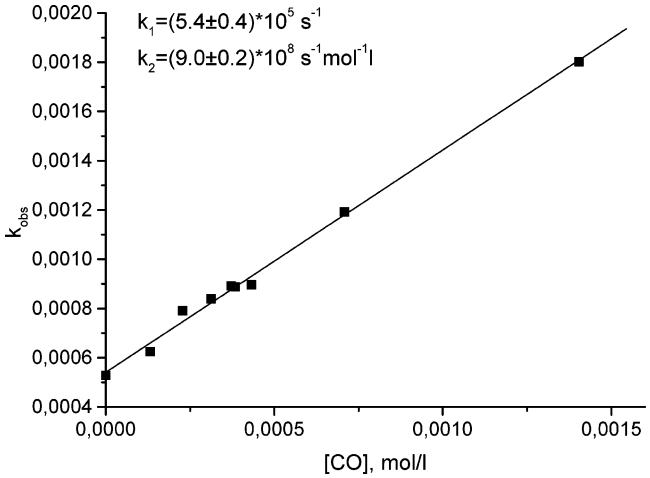

Figure 6. Dependence of the transient I decay rate constant on CO concentration. Experimental data are given in black rectangles; the straight line represents the best linear fit.

Discussion

The above results can be discussed in terms of the following schematic reaction scheme

$$Rh_4(CO)_{12} \xrightarrow{h\nu} \ldots \xrightarrow{\text{fast}} \text{Tr I} \xrightarrow{\text{slow}} \text{Tr II} \xrightarrow{\text{slow}} Rh_4(CO)_{12}$$

Absorption of light at 266 or 355 nm results in the eventual formation of I, which decays to form II, after which II decays to reform $Rh_4(CO)_{12}$. The instrumental time resolution does not allow the observation of intermediates preceding transient I on times shorter than 20 ns. Such subnanosecond processes will surely include vibrational relaxation of the molecular excited state as well as various ligand sphere and solvent shell reorganizations. However, on the basis of the data obtained, we believe that transients I and II are responsible for the reactivity of $Rh_4(CO)_{12}$ in the substitution photochemistry of this cluster.

Monitoring the reaction course using FTIR spectrometry allows structural characterization of both transients. The spectrum in Figure 3 is an average of the first 10 time slices (10 μs) after excitation. The positive absorption bands are assigned to correspond to vibrational transitions in I (see also Table 1). An analogous procedure for the last 10 slices of the same data sets yielded the spectrum shown in Figure 4. The positive absorption

TABLE 1: IR Spectral Bands of Transients I and II Obtained from Difference TR IR Spectra

Tr I, ν(CO), cm^{-1}, heptane	Tr II ν(CO), cm^{-1}, heptane	$Rh_4(CO)_{11}PPh_3$[a] ν(CO), cm^{-1}, hexane
	2093 w	2088 m
2054 vs	2060 vs	2058 vs
2036 m	2037 m	2032 s
	2027 m	2025 sh
2009 w	2014 w	2015 sh
1902 m	1876 m	1876 m
1866 m	1858 m	1856 m

[a] The spectrum was recorded using a sample of $Rh_4(CO)_{11}PPh_3$ synthesized according to a literature procedure.

bands are assigned to vibrational transitions in II, which has been generated from I (see also Table 1). The spectral bands of transient II lead to an assignment of its structure, based on similarity of this IR pattern with those obtained for structurally and spectroscopically characterized $Rh_4(CO)_{11}(L)$ clusters where L = PPh_3, $P(OPh)_3$.[22,23] The relative positions and intensities of the bands attributed to II closely match the features of the IR spectra of the $Rh_4(CO)_{11}(L)$ derivatives, in which the phosphine heteroligands occupy an axial site at rhodium atoms in the basal (CO-bridged) triangle of the metal tetrahedron. Comparison of columns 2 and 3 in Table 1 shows the strong similarity between the $Rh_4(CO)_{11}PPh_3$ spectrum and that assigned to II. Taking into account the high sensitivity of the IR patterns of carbonyl clusters to the degree of CO ligand substitution and the location of the heteroligand (i.e., the symmetry of the CO environment), it is reasonable to conclude that II has the $Rh_4(CO)_{11}$(solv) composition and the structure schematically shown in Figure 3, where the solvent molecule occupies an axial position in the CO-bridged cluster face. These observations clearly indicate that irradiation into the MLCT band of $Rh_4(CO)_{12}$ eventually results in the dissociation of a CO molecule, leading to a solvent-substituted intermediate that is structurally closely analogous to ground-state monosubstituted derivatives of this cluster. This type of the photochemical behavior has been observed earlier for the tri-[2,3,8,11,18] and tetranuclear[4,5] carbonyl clusters and it is believed to be responsible for the photosubstitution and photocatalytic reactions of these transition metal complexes.

That the IR spectrum attributed to transient I is quite different from that of II evidently points to substantial differences in the structure of the carbonyl environment caused by the transformation of I into II. The kinetics of this I → II transformation were single exponential and consistent with an intramolecular process. It seems likely that I is an isomer of II with a different disposition of coordination vacancy occupied by a solvent molecule. The presence of both terminal (2054, 2036, 2009 cm^{-1}) and edge-bridging (1902 and 1866 cm^{-1}) carbonyl frequencies in the spectrum of I as well as their location at approximately the same spectral intervals as those found for II suggests that the most probable alternative structures for I are those shown Figure 3. In these structures the solvent molecule might occupy either a radial vacancy in the basal rhodium triangle or a coordination vacancy at the apical rhodium atom. The transformation of the transient I into II can be described in terms of the solvent molecule migration accompanied by rearrangement of the carbonyl environment around the tetrarhodium skeleton. A closely analogous isomerization reaction has been reported in $Ir_4(CO)_{11}\{P(OR)_3\}$ clusters[24] by means of ^{13}C and ^{31}P NMR spectroscopy. In that case the phosphite ligands exchanged between axial and equatorial positions at the basal (CO-bridged) triangle via carbonyl ligand movements, which eventually changed the location of the bridged triangle, thereby changing the stereochemical position of the phosphite ligand. The mechanism of such exchange can be described in terms of an "all terminal" intermediate,[24] which has been shown to be operative in the case of thermal CO scrambling in the parent $Rh_4(CO)_{12}$ cluster.[25] This type of intramolecular dynamics is universally accepted as the description of isomerization and scrambling processes in transition metal carbonyl clusters and it is proposed that a similar mechanism is operative here.

It is also noteworthy that the independently determined rate of CO ligand scrambling in the ground-state $Rh_4(CO)_{12}$ species[25] is in good agreement with the lifetime of the I−II transformation. The room-temperature rate constant of CO migration around the Rh_4 skeleton as determined by dynamic ^{13}C NMR spectroscopy[25] was 1.29×10^6 s^{-1}. This is less than 3 times slower than the dynamics of the observed I → II rearrangement. As mentioned above, the mechanisms of both processes can be described in analogous ways and similarity of the kinetic parameters found for these dynamics supports strongly the chemical models suggested for the structures of transients I and II and their transformations in solution. It seems possible that the slightly higher reactivity of I in an essentially similar process is due to the presence of a "lightly bound" solvent molecule in the coordination sphere of this species.

In the reaction of I with CO, the concentration dependence of k_{obs} can be expressed by the usual competition kinetics expression, viz.

$$k_{obs} = k_1 + k_2[CO] \quad (1)$$

In accord with eq 1 the values of k_{obs} were linear with [CO] (Figure 6). From the linear plot, values of $k_1 = (5.4 \pm 0.4) \times 10^5$ s^{-1} and $k_2 = (9.0 \pm 0.2) \times 10^8$ M^{-1} s^{-1} were extracted. The CO-independent rate constant (k_1) extrapolated from the regression analysis is in good agreement with the direct observation of the decay of transient I (Figure 5), as required by the arguments invoked above. The bimolecular rate constant, k_2, arises from the trapping of transient I by CO to give the starting $Rh_4(CO)_{12}$ cluster. Under the conditions of excess substituted ligand (solvent), both dissociative and associative channels yield first order dependence on the CO concentration. However, a dissociative mechanism seems to be more probable compared to an associative substitution because of the very weak coordination of hydrocarbon molecules in transition metal complexes. The value of $k_2 = (9.0 \pm 0.2) \times 10^8$ s^{-1} M^{-1} is very close to the bimolecular rate constant obtained for the trapping of the photogenerated $\{Ru_3(CO)_{11}\}$ dissociative species (2.4×10^9 s^{-1} M^{-1}) by CO in hydrocarbon solvents.[18]

The proposed reaction sequence for the photoinitiated transformations of the $Rh_4(CO)_{12}$ cluster on the nanosecond time scale is

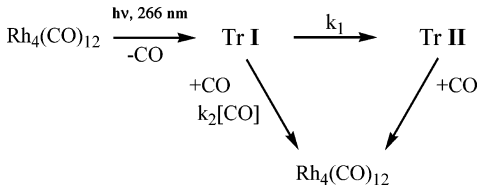

The absence of the transient I scavenging by CO in the experiments without addition of free CO to the starting solution can be explained by the relative magnitudes of the k_1 and k_2[CO] terms in eq 1 when the only source of CO concentration arises from the photodissociation reaction. The typical value of [CO] generated from the reactant under flash photolysis condi-

tions would be near 10 μM. Combining this with $k_2 \sim 10^9$ M^{-1} s^{-1} yields a k_2[CO] term of $\sim 10^4$ s^{-1}, some 50× less than the value found for k_1. Thus the first term on the RHS of eq 1 dominates and the decay of I shows no second order contribution. Transient II is substantially longer lived and apparently reacts with CO to regenerate the starting material as its sole reaction product.

One of the most interesting features of the scheme given above is that photodissociation of CO occurs from a position different from that normally observed in thermal substitution reactions. The relaxation of excited species (in the absence of substituting ligands) results in an isomerization process to give a stabilized (thermodynamic) structure. However, it is possible to trap nonequilibrium structures provided that an excess of substituting species is presented and the isomerization of coordination sphere is frozen in one way or another. This observation shows that, at least in principle, photochemistry may give rise to unusual structures and reactivity patterns, which are different of those generated in thermal reactions and elucidation of mechanistic features of the fast photoreaction stages is of critical importance for understanding and exploitation of this chemistry.

Supporting Information Available: A perspective view of a typical dynamic surface, $A(\bar{\nu},t)$, is shown in Figure S1. This material is available free of charge via the Internet at http://pubs.acs.org.

References and Notes

(1) Braunstein, P.; Oro, L.; Raithby.; P. R. *Metal clusters in Chemistry*; Wiley-VCH: Germany, 1999.

(2) Bentsen, J. G.; Wrighton, M. S. *J. Am. Chem. Soc.* **1987**, *109*, 4530.

(3) Bentsen, J. G.; Wrighton, M. S. *J. Am. Chem. Soc.* **1987**, *109*, 4518.

(4) Bentsen, J. G.; Wrighton, M. S. *J. Am. Chem. Soc.* **1984**, *106*, 4041.

(5) Yamamoto, S.; Asakura, K.; Mochida, K.; Nitta, A.; Kuroda, H. *J. Phys. Chem.* **1993**, *97*, 565.

(6) Malito, J.; Markieviwicz, S.; Poë, A. J. *Inorg. Chem.* **1982**, *21*, 4335.

(7) Brodie, N. M. J.; Huq, R.; Malito, J.; Markiewicz, S.; Poë, A. J.; Sekhar, V. C. *J. Chem. Soc., Dalton Trans.* **1989**, 1933.

(8) Desrosiers, M. F.; Wink, D. A.; Ford, P. C. *Inorg. Chem.* **1985**, *24*, 1.

(9) Desrosiers, M. F.; Wink, D. A.; Trautman, R.; Friedman, A. E.; Ford, P. C. *J. Am. Chem. Soc.* **1986**, *108*, 1917.

(10) Friedman, A. E.; Ford, P. C. *Photochem. Photophys. Coord. Compd., [Proc. Int. Symp.], 7th* **1987**, 217.

(11) Ford, P. C.; Friedman, A. E.; Taube, D. J. *ACS Symp. Ser.* **1987**, *333*, 123.

(12) Ford, P. C. *J. Organomet. Chem.* **1990**, *383*, 339.

(13) Nijhoff, J.; Bakker, M. J.; Hartl, F.; Stufkens, D. J.; Fu, W.-F.; van Eldik, R. *Inorg. Chem.* **1998**, *37*, 661.

(14) Tro, N. J.; King, J. C.; Harris, C. B. *Inorg. Chim. Acta* **1995**, *229*, 469.

(15) Vlček, A. M. *Inorg. Chem.* **1992**, *4*, 218.

(16) Vlček, A., Jr. *Coord. Chem. Rev.* **2000**, *200*−*202*, 933.

(17) Vlček, A., Jr.; Farrell, I. R.; J., L. D.; Matousek, P.; Tovrie, M.; Parker, A. W.; Grills, D. C.; George, M. W. *J. Chem. Soc., Dalton Trans.* **2002**, 701.

(18) Dibenedetto, J. A.; Ryba, D. W.; Ford, P. C. *Inorg. Chem.* **1989**, *28*, 3503.

(19) Fedorov, A. V.; Danilov, E. O.; Merzlikine, A. G.; Rodgers, M. A. J.; Neckers, D. C. *J. Phys. Chem.*, in press.

(20) Seidel, A.; Linke, W. *Solubilities of Inorganic and Metal Organic Compounds*, 4th ed.; D. van Nostrand Co.; New York, p 456.

(21) Holland, G. F.; Ellis, D. E.; Tyler, D. R.; Gray, H. B.; Trogler, W. C. *J. Am. Chem. Soc.* **1987**, *109*, 4276−81.

(22) Heaton, B. T.; Longhetti, L.; Mingos, D. M. P.; Briant, C. E.; Minshall, P. C.; Theobald, B. R. C.; Garlaschelli, L.; Sartorelli, U. *J. Organomet. Chem.* **1981**, *213*, 333−50.

(23) Tunik, S. P.; Haukka, M.; Nordlander, E. Synthesis and spectroscopic characterization of $Rh_4(CO)_{11}(Ph_2PThienyl)$ cluster. Unpublished results.

(24) Besancon, K.; Laurenczy, G.; Lumini, T.; Roulet, R.; Gervasio, G. *Helv. Chim. Acta* **1993**, *76*, 2926.

(25) Besancon, K.; Laurenczy, G.; Lumini, T.; Roulet, R.; Bruyndonckx, R.; Daul, C. *Inorg. Chem.* **1998**, *37*, 5634.